

# Intrinsic Camera Resolution Measurement

Peter D. Burns<sup>a</sup> and Judit Martinez Bauza<sup>b</sup>

<sup>a</sup>Burns Digital Imaging LLC, <sup>b</sup>Qualcomm Technologies Inc.

## ABSTRACT

Objective evaluation of digital image quality usually includes analysis of spatial detail in captured images. Although previously-developed methods and standards have found success in the evaluation of system performance, the systems in question usually include spatial image processing (e.g. sharpening or noise-reduction), and the results are influenced by these operations. Our interest, however, is in the intrinsic resolution of the system. By this we mean the performance primarily defined by the lens and imager, and not influenced by subsequent image processing steps that are invertible. Examples of such operations are brightness and contrast adjustments, and simple sharpening and blurring (setting aside image clipping and quantization). While these operations clearly modify image perception, they do not in general change the fundamental spatial image information that is captured.

We present a method to measure an intrinsic spatial frequency response (SFR) computed from test image(s) for which spatial operations may have been applied. The measure is intended ‘see through’ operations for which image detail is retrievable but measure the loss of image resolution otherwise. We adopt a two-stage image capture model. The first stage includes a locally-stable point-spread function (lens), the integration and sampling by the detector (imager), and the introduction of detector noise. The second stage comprises the spatial image processing. We describe the validation of the method, which was done using both simulation and actual camera evaluations.

**Keywords:** image resolution, intrinsic resolution, retrievable resolution, MTF, SFR, computational camera

## 1. INTRODUCTION

There are several well-established methods for measuring the capture of image detail, including those based on test objects containing elements such as edges, lines, sine-waves and random patterns. The resulting measure of the system’s ability to capture image detail is often expressed as a function of spatial frequency. While the origin of such measures is in linear-system analysis, it is understood that for practical imaging systems there is no unique Modulation Transfer Function (MTF). However, useful spatial frequency response (SFR) measures have been developed as part of imaging standards. Examples of these are the edge-SFR [1], and S-SFR [2] (based on a polar sine-wave feature) in the revised ISO 12233 standard [3]. A more recently-developed measure of image-texture capture is based on pseudo-random objects (e.g. circles) in a ‘dead-leaves’ pattern [4].

Our interest is in the *intrinsic* resolution of the system. By this we mean the performance primarily defined by the lens and imager, and not influenced by subsequent image processing steps that are invertible. Evaluation of this fundamental performance is important, for example, when evaluating and comparing image-capture systems which employ different image processing. For the analysis and comparison of both conventional and computational camera systems where it is not practical to disable the image processing, we need a method based on processed images.

We describe a method to measure an intrinsic SFR computed from test image(s) for which spatial operations may have been applied. As an example, consider image capture by an ordinary camera followed by a digital image sharpening operation. Using established SFR methods and comparing results for the same camera with and without filtering would yield different results. However, since the lens and imager have not changed and the filtering is invertible, we seek a method for which the two intrinsic SFR results are equivalent. In addition, for operations for which there is loss of spatial information, the desired method would indicate this reduction. In other words, the measure would ‘see through’ operations for which image detail is retrievable, but measure the loss of image resolution otherwise. For this method we adopt a two-stage image capture model.

In keeping with several previous measures of image structure, we base our analysis on the luminance image array that can be computed from a weighted sum of red, green and blue color-records for the camera. While we expect and observe differences in imaging performance between color-channels, we will not address these here.

## 2. TWO-STAGE SYSTEM MODEL

Before describing the method for measuring intrinsic camera resolution, we introduce a two-stage imaging model. This provides a simple description of the spatial image capture characteristics, and provides a basis for the method. Consider Fig. 1 which shows the elements of the model. The first stage includes a locally-stable point-spread function (lens), the integration and sampling by the detector (imager), and the introduction of detector noise. The second stage comprises the spatial image processing. Since the image processing is not restricted to linear operations, this model is used with the understanding that its parameters will approximate the corresponding measures for an ideal model system. The method is based on cascaded linear operations,  $h_1$  and  $h_2$ , and a stochastic noise source,  $n$ . We interpret  $h_1$  as describing the lens and detector, and  $h_2$  the image processing.

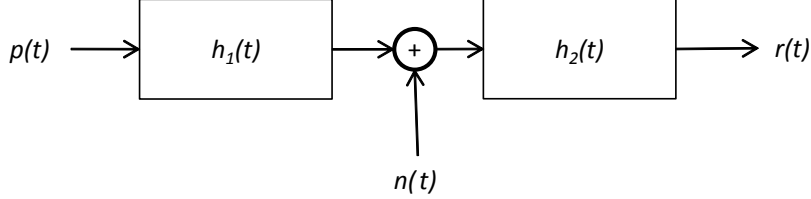


Figure 1: Two-stage model

Based on the two stages of our model, described by effective point-spread functions  $h_1$  and  $h_2$ , we can introduce the corresponding modulation transfer functions. These are the corresponding moduli of the Fourier transforms

$$H_1 = |FT[h_1]|, \quad H_2 = |FT[h_2]| \quad (1)$$

where  $FT$  indicates the Fourier transform and  $|\bullet|$  the modulus, or magnitude, of a complex function. Furthermore, we will assume that these two functions cascade to form the system MTF

$$H = H_1 H_2. \quad (2)$$

If an input signal is  $p(t)$  the corresponding output is given by

$$r(t) = [p(t) * h_1(t) + n(t)] * h_2(t) \quad (3)$$

where  $*$  indicates convolution and  $n(t)$  is the detector noise expressed as an array.

Since the camera noise is modelled as being at least partly stochastic, we normally express signal and noise transfer in terms of power-spectral densities<sup>†</sup>

$$\Phi_{rr}(u) = [\Phi_{pp}(u)H_1^2(u) + \Phi_{nn}(u)]H_2^2(u) \quad (4)$$

where  $\Phi_{pp}$ ,  $\Phi_{rr}$  and  $\Phi_{nn}$  are the spectral density functions for input signal, output image and detector noise, respectively.

### 2.1 Two-stage model based resolution measure

As stated above,  $H_1$  is the effective MTF due to the lens and detector. Therefore, if it were possible to estimate  $H_1$  from observations of input  $p(t)$  (a test object or target), and  $r(t)$  (the output image array), then we would have a measure of the intrinsic resolution of the system. Our system model provides us the framework. From Eq. (4) we can express the system output spectrum as the sum of two components

<sup>†</sup> The power-spectral density is often called the noise-power spectrum, however we avoid the term because we will be considering both signal- and noise-spectra.

$$\Phi_{rr}(u) = \Phi_{rr\_signal} + \Phi_{rr\_noise} \cdot \quad (5)$$

The output *signal* spectrum that would be observed in the absence of detector noise (we are not assuming this would be possible) is

$$\begin{aligned} \Phi_{rr\_signal}(u) &= \Phi_{pp}(u)H^2(u). \\ \Phi_{rr\_signal}(u) &= \Phi_{pp}(u)H_1^2(u)H_2^2(u). \end{aligned} \quad (6)$$

We can also express signal transfer in terms of the cross-spectrum (see Appendix, Eq. 2a)

$$\Phi_{pr\_signal}(u) \cong \Phi_{pp}(u)H_1(u)H_2(u) \quad (7)$$

Using the cross-spectrum for SFR estimation can reduce the bias due to image noise that is seen in auto-spectral methods. However it is computationally more demanding, as we will see below.

The output noise spectrum is

$$\Phi_{rr\_noise}(u) = \Phi_{nn}(u)H_2^2(u). \quad (8)$$

These equations can now be used to describe the general form of the intrinsic resolution measurement. Using Eq. (2), we first solve Eq. (7) for the system (signal) MTF

$$H(u) = \frac{\Phi_{pr\_signal}(u)}{\Phi_{pp}(u)} \quad (9)$$

As indicated in Eq. (2),  $H(u)$  is the cascaded system MTF however we are interested in  $H_1(u)$

$$H_1(u) = \frac{H(u)}{H_2(u)}. \quad (10)$$

So if the system  $H(u)$  can be measured by Eq. (9) and the (spatial) image processing MTF,  $H_2(u)$  can be measured, then the lens-detector (intrinsic) MTF can be estimated using Eq. (10). Eq. (7) can be solved for  $H_2(u)$

$$H_2(u) = \left[ \frac{\Phi_{rr\_noise}(u)}{\Phi_{nn}(u)} \right]^{0.5}. \quad (11)$$

This expression can be substituted into Eq. (10) to yield the desired  $H_1(u)$ . In summary, a method based on these model relationships requires information or measurement of the following

$\Phi_{rr\_signal}$  : output signal spectrum

$\Phi_{nn}$  : detector noise spectrum

$\Phi_{rr\_noise}$  : output noise spectrum

We now turn from model equations which motivate the form of the measurement method, to practical statistical estimates of these parameters.

### 3. METHOD

In keeping with the language used in most digital camera standards, we will refer to the measured, or estimated, signal transfer functions as spatial frequency responses (SFRs) to differentiate them from unique model MTFs for linear systems and sub-systems. The cameras whose performance we intend to measure include various image processing

operations which can adapt to scene information. In this case we select a test target with spatial characteristics similar to actual scenes. We use texture-based test targets, such as the *dead-leaves* test chart, consisting of a random distribution of gray circles. To assess the generality of the method, however, we also use other test patterns, including one that emphasizes edge information. *Zentangle Square 2*, by Penny Raile, is included in the center of our *Edges* test target. Both targets are shown in Fig. 2.

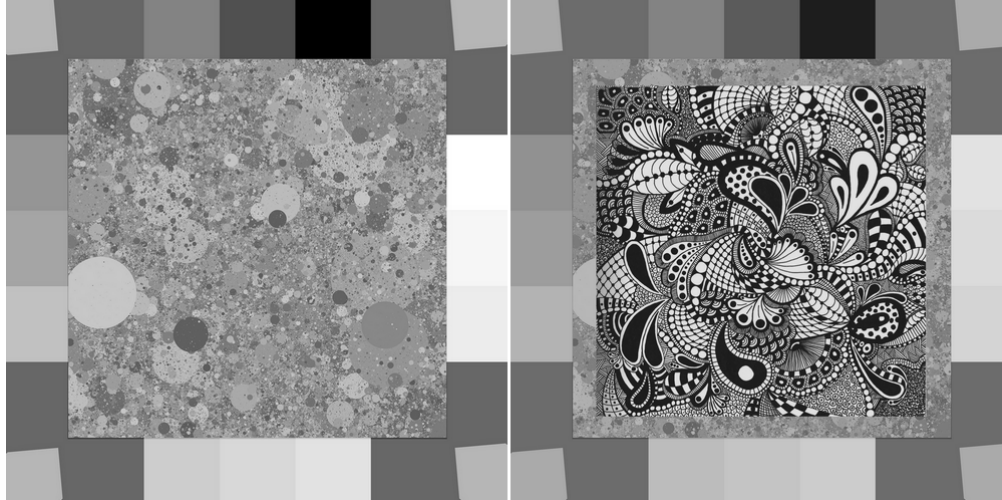


Figure 2: Test targets used to validate method: Dead-leaves and Edges (center region is courtesy of Penny Raile)

As described above, we need a method that provides estimates of both signal and noise spectra which are derived solely from input and output image information. To accomplish this we acquire several replicate images of the test target. The intent being, that these registered sets can be used to estimate the temporal image noise from which we can estimate both output signal and noise spectra.

### 3.1 Input data sets

An outline of the intrinsic SFR method is shown in Fig. 3. There are two sets of input data needed.

1. Scanned image file from the test target used. This is needed for the cross-spectral analysis used for the signal spectrum estimation, described below.
2. Set of  $N$  replicate test images from the camera being evaluated. We found success with  $N$  equal to ten, although the exact number is not critical.

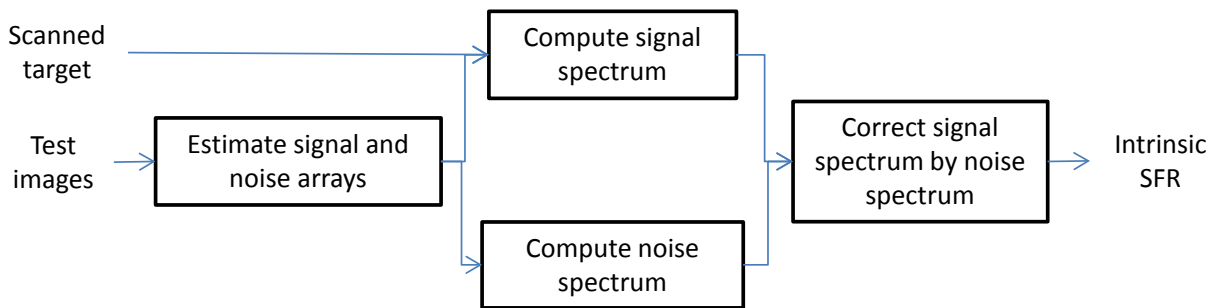


Figure 3: Outline of the method

### 3.2 Computing the signal and noise arrays

From the set of  $N$  replicate test images we derive a mean ‘signal’ image array and  $N$  corresponding ‘noise’ arrays. The first step is to automatically register the test image arrays. This was found to be necessary even with the use of a camera

tripod. From the set of registered images, the mean array is taken as the signal array. For a set of  $N$  registered ( $P \times R$ ) images,  $r_{i,j,n}$  where the indices are for pixel, row and frame, respectively, the signal array is

$$r\_signal_{i,j} = \frac{1}{N} \sum_{j=1}^N r_{i,j,n}. \quad (12)$$

The set of  $N$  estimated noise arrays are computed as the pixel-by-pixel differences from this compute mean signal array

$$r\_noise_{i,j,n} = r_{i,j,n} - r\_signal_{i,j}. \quad (13)$$

### 3.3 Computing the signal spectrum

For most imaging applications, the power-spectral density measurement calls for an auto-spectral estimate. The power-spectral density for a stochastic process is defined as the Fourier transform of the spatial auto-covariance function, or when normalized by the variance, the auto-correlation. There are several methods for estimating the power-spectral density from sampled data, but we adopt one based on a single Discrete Fourier transform followed by a radial averaging that has been used frequently in digital camera evaluation techniques, such as those for image texture [6].

For each of the auto- or cross-spectrum estimates, the first step is to fit and subtract a two-dimensional plane to the image data of the selected analysis region. This de-trending step significantly improves the low-frequency spectrum estimation [6]. To demonstrate this Fig. 4 addresses a nominally uniform region from one of our camera test images. The left-hand plot shows the 150 x 150 pixel region, with the computed two-dimensional linear (plane) function that was fit to the data (on the right). Note that the z-axis is different for these plots to exaggerate the slope of the fitted function. A simple least-square polynomial fitting method was used.

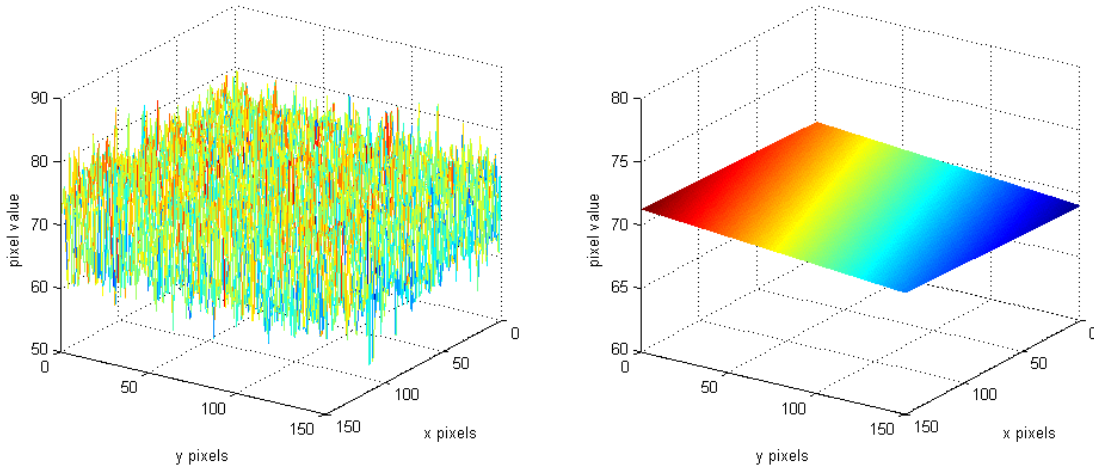


Figure 4: Example of nominally uniform image region and the two-dimensional fit used for de-trending

The spectral estimation methods described in this report, and generally used for imaging performance evaluation, assume stationary statistics for the sample data sets. Evaluation of the power-spectral density is an analysis of the second-order (variance) statistics of the data. Unwanted variation of the mean, *i.e.* a long-term trend, over the data set can cause a bias in the estimate, particularly at low spatial frequencies. Before computing the spectrum, we apply the simplest and most benign corrections to sample data by subtracting the plane that is fitted to the sample image. An example of this is shown in Fig. 5, where we plot the one-dimensional power spectral density based on the data of Fig. 4, with and without this de-trending step. Note the increase (bias) introduced at low spatial frequencies by this apparently minor trend in the data. This subject is discussed more fully in Ref. [6].

For an ( $N \times N$ ) luminance image array, the auto-spectrum estimate is computed as the square of the amplitude of the two-dimensional DFT of the array, e.g.,

$$S_{pp}(m,n) = |DFT[p(x,y)]|^2 \quad (14)$$

where the  $(N \times N)$  luminance image array data are,  $p(x, y)$ , corresponding to, e.g., the dead leaves region, and  $DFT$  is the Discrete Fourier Transform.

As described in the Appendix, however, we can derive a measure of signal transfer without the bias introduced by the detector noise using a cross-spectral estimate, recently described by Kirk, *et al.* [5]. The cross-spectrum is computed as

$$S_{pr}(m, n) = \left| DFT[p(x, y)] DFT^*[r(x, y)] \right| \quad (15)$$

where  $p$  is the input test target array and  $r$  the captured image. From this two-dimensional cross-spectrum we compute a smoothed, one-dimension estimate by radial averaging

$$S_{pr\_signal}(u)$$

where  $u = (m^2 + n^2)^{0.5}$  the radial frequency index  $v = 1, 2, \dots, v_{\max}$ .

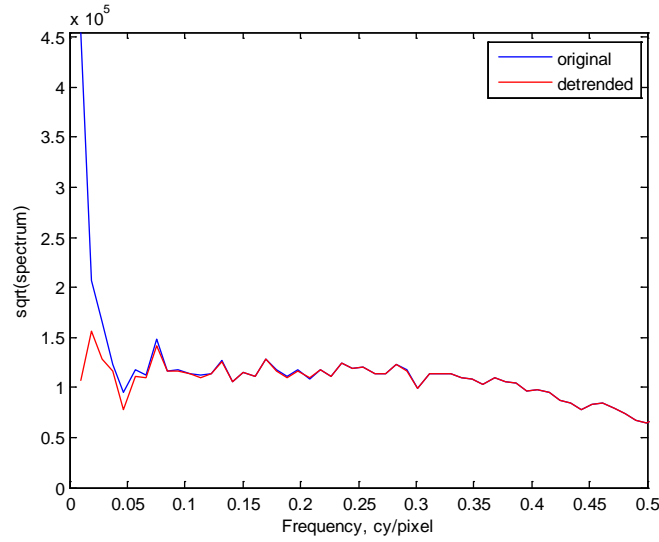


Figure 5: Example of the influence of a long-term data trend on spectral density estimates. The square-root of the spectrum is plotted with and without the subtraction of the fitted function

### 3.4 Computing the noise spectrum

From the set of computed image noise arrays, using Eq. (13), the auto-spectrum is computed as in Eq. (14). Following the radial frequency-averaging the mean noise spectrum estimate is

$$S_{pr\_noise}(u) = \frac{1}{N} \sum_{i=1}^N S_{pr\_noise,i}(u). \quad (16)$$

### 3.5 Computing of intrinsic resolution SFR

The first step is to compute the signal transfer SFR, as in Eq. (9)

$$\hat{H}(u) = \left[ \frac{S_{pr\_signal}(u)}{S_{pp}(u)} \right] \quad (17)$$

which corresponds to our estimate of  $H(u)$ . In order to measure the intrinsic SFR as in Eq. (10) we need to estimate  $H_2(u)$ . This can be done by using Eq. (11) but requires that we know the power spectral density of the detector noise source. This is not available directly, but we can assume (or determine independently) the spectrum *shape*. In many

cases the detector noise can be described as a spatially uncorrelated noise source. In this case we can take the estimated  $H_2(u)$  as

$$\hat{H}_2(u) = \left[ \frac{S_{rr\_noise}(u)}{S_{rr\_noise}(\sim 0)} \right]^{0.5} \quad (18)$$

where the denominator is computed as the average spectrum value near zero-frequency. The intrinsic SFR is then computed from the results above results, following Eq. (10)

$$\hat{H}_1(u) = \frac{\hat{H}(u)}{\hat{H}_2(u)}. \quad (19)$$

#### 4. VALIDATION

To test the intrinsic SFR method, we applied it in several experiments, outlined in Fig. 6. Both test targets shown in Fig. 2 were printed to a size of 21 cm x 21 cm (8.26 x 8.26 inches). These printed targets were then scanned at a sampling resolution consistent with the corresponding test images from the camera under test. This was done to simplify the analysis because there would then be no need to resample the target image to match the test image array data. Using the scanned target image data also eases the requirements for the printer used for the targets. As an example of the image sampling parameters, the camera under test was a Nikon 3000 DSLR, with captured images of 3972 x 2592 (10.3 MP).

Images were captured with two test targets side-by-side, so that each one spanned a region of 1500 x 1500 pixels. This resulted in an image sampling on the target of

$$1500 \text{ pixels}/8.26 \text{ inches} = 181 \text{ pixels/inch.}$$

This was the sampling used for the scanning of the test targets with the Epson Perfection V600 scanner.

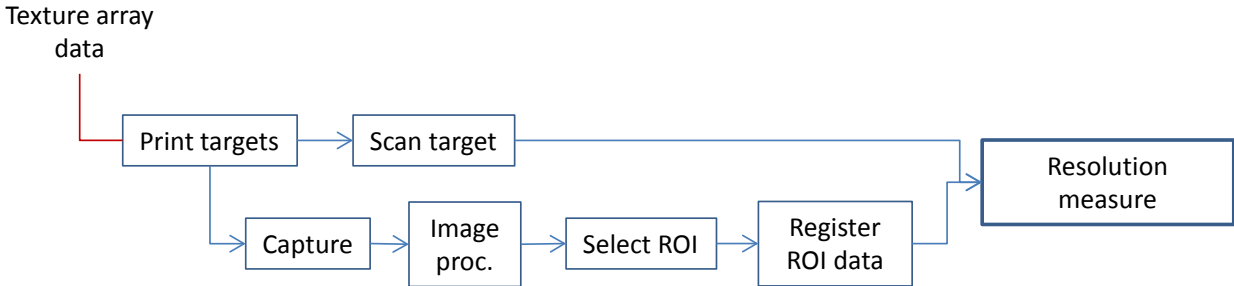


Figure 6: Outline of method as applied to camera evaluation

*Scanner MTF:* The scanned image of the printed target becomes the input for our analysis. This means that it is possible that the scanner performance can influence the results. However, measuring the scanner MTF can be used to assess its influence and, if necessary, compensate for it. A reference photographic test target was scanned with the same parameters (16-bit, tiff, 180 pixels/inch). From an edge feature, the scanner MTF was computed and is plotted in Fig. 7. Note that the MTF is above 80% for the frequency range covered by our subsequent camera evaluation. Therefore we observe that the scanner performance does not have a large influence the measurement of our input test target.

*Camera Files:* For our testing, several sets of Nikon camera raw image files were captured. The raw format was used in order to avoid the influence of jpeg compression, which would normally be imposed on delivered images. The lens autofocus function was used, and image sets were capture with a range of camera ISO settings (ISO 200 – ISO 1600).

After the scanned target and camera image files were acquired and selected, an image sub-region that would be used for the analysis was selected. We have tested the method for several square region sizes, with reliable results observed for regions of at least 400 x 400 pixels. Each of the corresponding regions for the test images was brought to a common registration using a simple x-y translation algorithm. The set of registered test regions and the corresponding scanned target region were then taken as input to the intrinsic SFR measurement method described in Fig. 6.

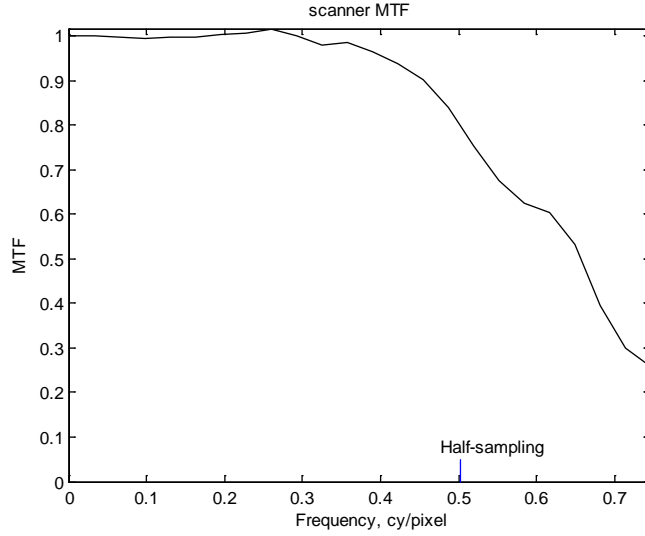


Figure 7: Scanner edge-MTF as measured from a reference photographic target

### Experiment 1: Camera

Our first example is for a camera ISO 400 setting, using the moderate-contrast dead-leaves pattern. No post-processing of the images was performed, and the results are given in Fig. 8. In Fig. 8a, the blue line is for the (uncorrected) signal-transfer SFR,  $\hat{H}(u)$ , as in Eq. (17). Note that the corresponding estimate of  $\hat{H}_2(u)$ , Eq. (18), based on the normalized square-root of the noise spectrum has much less fall-off with frequency. This is to be expected, given that no filtering or noise-reduction has been applied to the test images. The resultant intrinsic SFR,  $\hat{H}_1(u)$  is given by the black line. Figure 8b re-plots this result, with a smoothed version. The smoothing of the intrinsic SFR vector was done using a simple fourth-order polynomial fit. This fit was not constrained to be unity at zero-frequency, although this is a logical next step. Also added in Fig. 8b is a signal SFR derived from a signal edge feature. Note that this results is similar to the intrinsic SFR, however is shows a higher response at high frequencies, possible due to image noise.

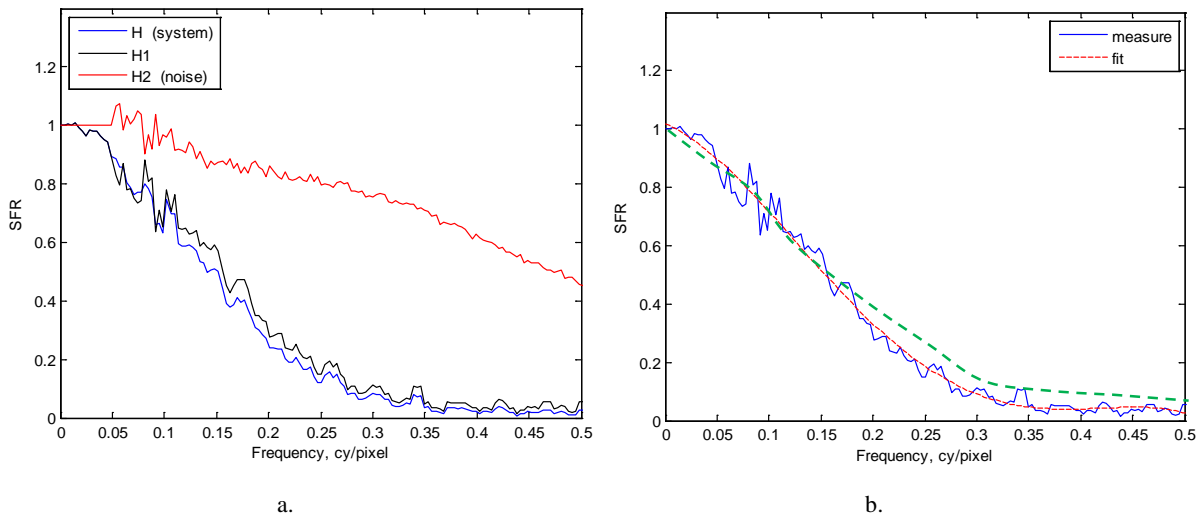


Figure 8: Results for Nikon 3000D camera (ISO 400) and no post-processing, (a) components (H1 is the computed intrinsic SFR) and (b) computed and smoothed result, with edge-SFR added as green dotted line.



### Experiment 2: Comparison of different test target content

It is common to use particular texture-based test targets for camera evaluation. This is important when the signal spectrum is assumed by the analysis method. This is the case when the dead-leaves pattern is used for the capture of image texture [4]. The particular function form of the dead-leaves pattern was chosen with the intent of achieving a ‘scale-independent’ method. When this is achieved, one would not need to know the exact image (spatial) sampling on the target. We do not consider this as a goal for our method, however, since the size of the printed target is known.

Furthermore, one of our objectives is to provide a method that is *not* dependent on any particular texture pattern. To assess the generality of the method, we used both test targets of Fig. 2 for our camera evaluation. The results of the camera evaluation based on the dead-leaves and edges targets are shown in Fig. 9. As intended, the results are in good agreement, with differences within measurement variability.

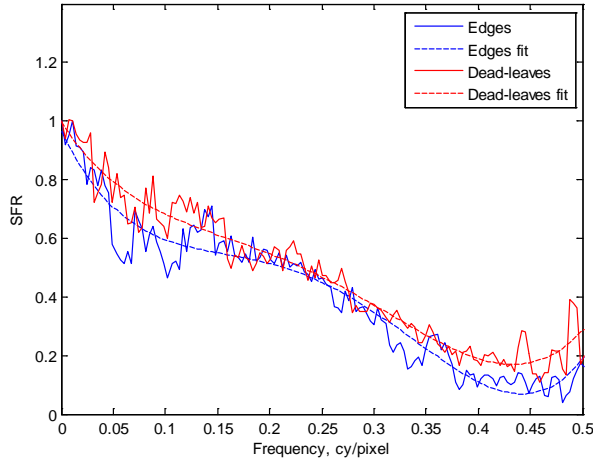


Figure 9: Comparison of intrinsic SFR results for the Nikon camera with ISO 200 for the two test targets of Fig. 2

### Experiment 3: Simple Sharpening

This example included two levels of image sharpening using an unsharp masking method. In this case we would expect the apparent signal-transfer to indicate a higher effective SFR, however, our intrinsic SFR should be virtually unchanged. Figure 10 shows results from slanted-edge analysis for the three conditions, no processing, moderate sharpening (radius 2, 50%) and high sharpening (radius 3, 100%). As we would expect, the results are directly influenced by the sharpening applied.

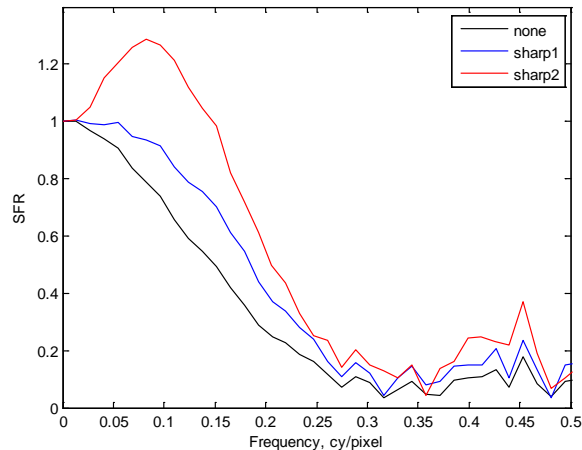


Figure 10: Edge-SFR results for the camera and following two levels of image sharpening

These results can be compared with the corresponding intrinsic SFR analysis shown in Fig. 11. In Fig. 11a and 11c the intermediate results are plotted. We see that both the uncorrected signal transfer and noise-based spectra are increased with image sharpening. As shown in Figs. 11b and 11d the resulting intrinsic SFR measurements, however, are largely

uninfluenced by the processing. So despite differences in signal and noise spectra, the intrinsic resolution is measured as equivalent. This is the intended result for our method, since this type of spatial filtering is reversible.

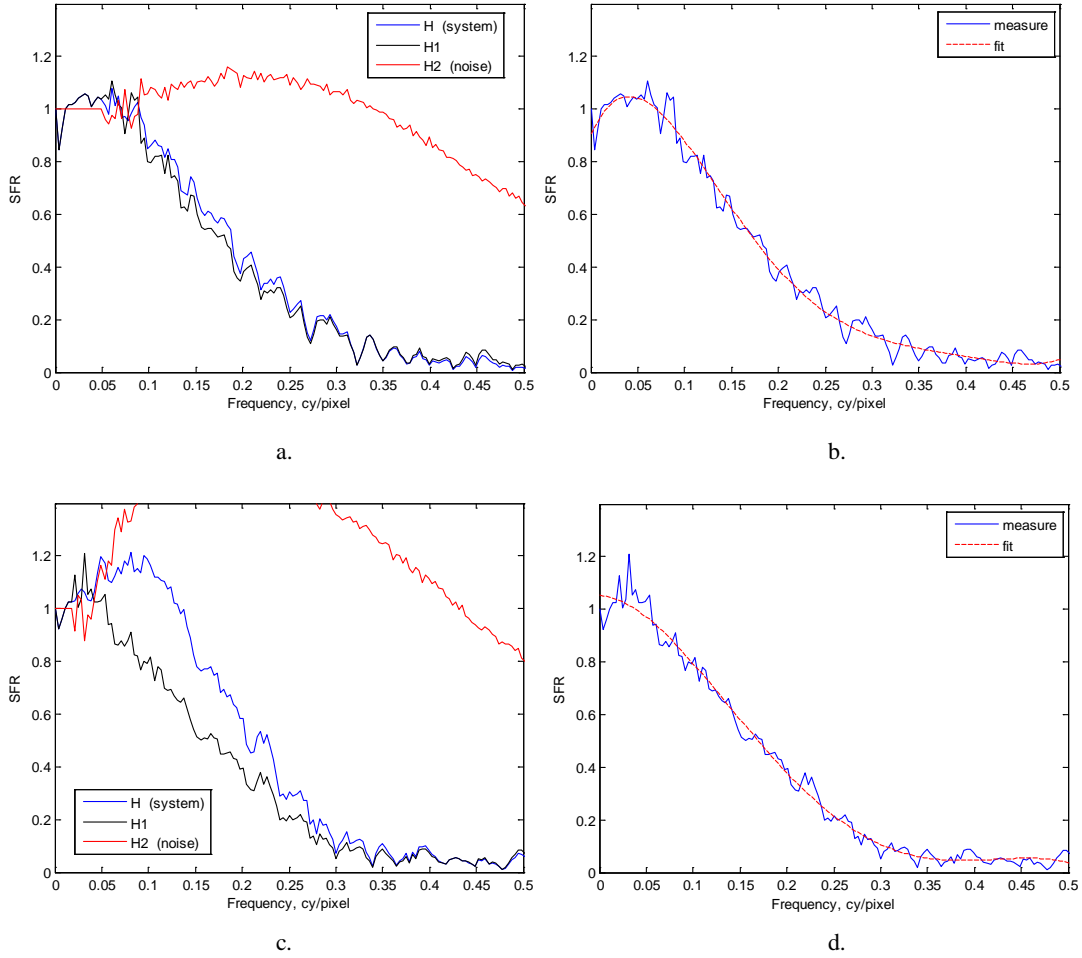


Figure 11: Results of intrinsic SFR analysis following two levels of image sharpening, (a, b) moderate (c, d) strong.

#### Experiment 4: Variability with Camera ISO Setting

Most standard methods for the evaluation of image (signal) performance are susceptible to image noise. This usually contributes both bias error, e.g. a noise floor in the edge-SFR, and variability. As described above, the intrinsic SFR method attempts to minimize the unwanted influence of image noise in two ways. Using the cross-spectrum method to estimate the signal transfer reduces the image noise component in the computed estimate. In addition, the computed correction term due to the spatial image processing,  $\hat{H}_2(u)$ , is based on a normalized noise spectrum, and therefore not proportional to the noise level introduced. To validate this approach and evaluate the extent of residual variation with noise level, the camera was tested over a wide range of ISO settings, for the same exposure level. The results are shown in Fig. 12, and indicate good agreement between camera settings. It should be noted that each of these measurements results from an independent analysis. The (400 x 400 pixel) image regions used for the analysis, although similar, were not identical. The results include statistical variation that is part of any spectral analysis.

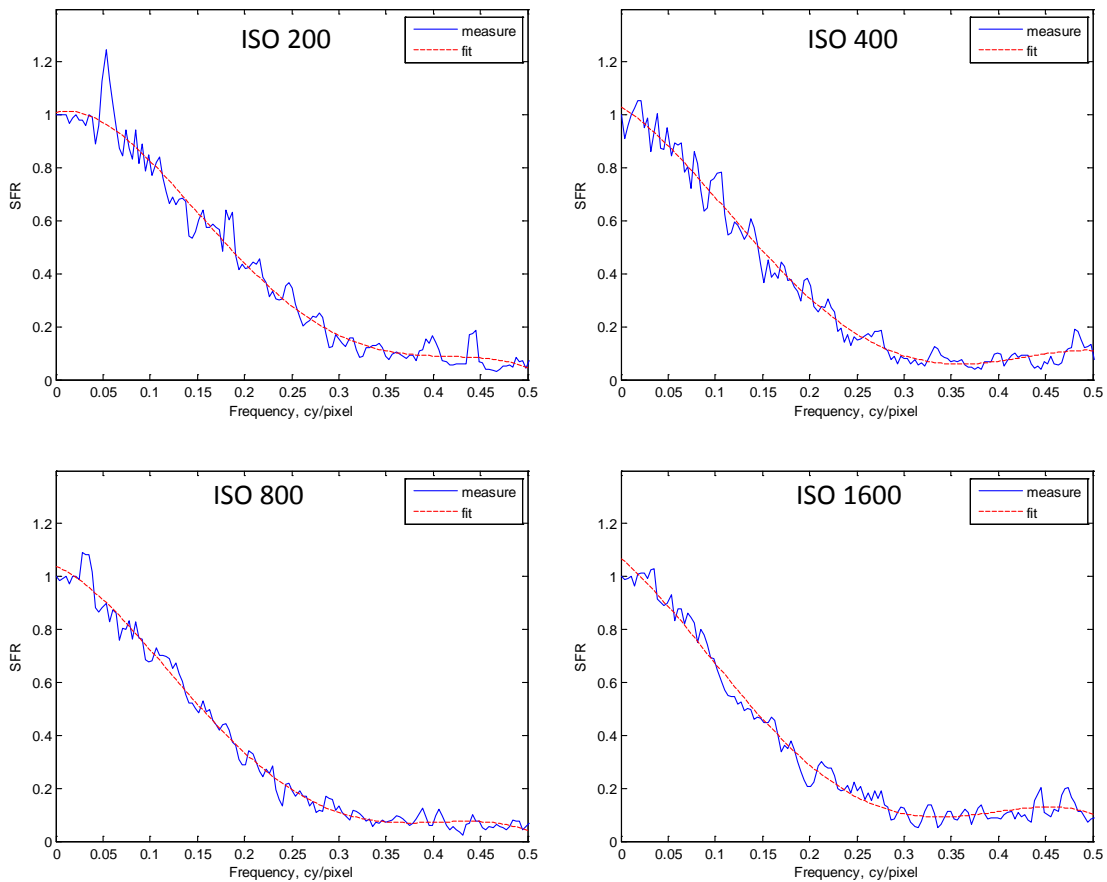


Figure 12: Intrinsic-SFR results for a range of camera ISO settings

### Experiment 5: Cascading of median filter with sharpening

In this example we process the captured images with a (5x5) median filter, followed by a linear sharpening filter. This is the same, strong sharpening filter that was used in example 3 above (radius 3, 100%). We would expect that the median filter, while reducing image noise, may also reduce the intrinsic image resolution. However, the subsequent (linear) sharpening operation should not further modify the SFR because it is reversible. Figure 13 shows the results for camera ISO 400 and the dead-leaves test target.

Figure 13a shows the results for the image capture with no post-processing. Following the median filter, Fig. 13b indicates some resolution loss as we would expect, with the superimposed red line indicating the location of the 20% camera response as a reference. However, despite the subsequent application of the sharpening filter, Fig. 13c shows no increase in intrinsic resolution. So this result is consistent with our objectives for the method.

## 5. SUMMARY

The method for measurement of the intrinsic resolution of digital cameras has been described. While the framework for the method is a simple two-stage image capture model, its application to general practical cameras and non-linear image processing has been demonstrated. Based on our implementation and validation process, we conclude that the following have been achieved:

- Reliable measurement using small areas (locality); this is useful for systems for which characteristics vary across the image field
- Robust (invariant) results for a range of camera ISO settings (200-1600)

- Stable results for different test-target texture patterns, due in part to the use of cross-spectral signal estimation
- For cases with no post processing, the intrinsic SFR compared favorably with edge-SFR for low-noise image capture
- For several levels of invertible operations (e.g. sharpening, contrast stretching) the desired results were achieved, *i.e.* equivalent intrinsic (retrievable) resolution was reported
- Desired loss of intrinsic resolution was reported for several imaging paths where expected, e.g., non-linear filtering
- Improved stability achieved via data de-trending, and automatic registration of the image regions of interest used for both cross-spectral signal and auto-spectral estimation

### Limitations to the method

The method is dependent on an assumption of uncorrelated, or of known correlation, stochastic noise, in order to estimate  $H_2$ . However, noise may not be of this kind. It is possible that fixed-pattern, temporal and periodic artifacts may be introduced. These can lead to unstable results. If  $H_2$  cannot be estimated reliably, then equation (10) cannot be solved for  $H_1$ . However, we did not find this to be a problem.

The second limitation is due to the nonlinear nature of the image processing steps that we are attempting to characterize. While we see stable results for several linear and non-linear operations others may introduce a signature into the estimated intrinsic resolution measure.

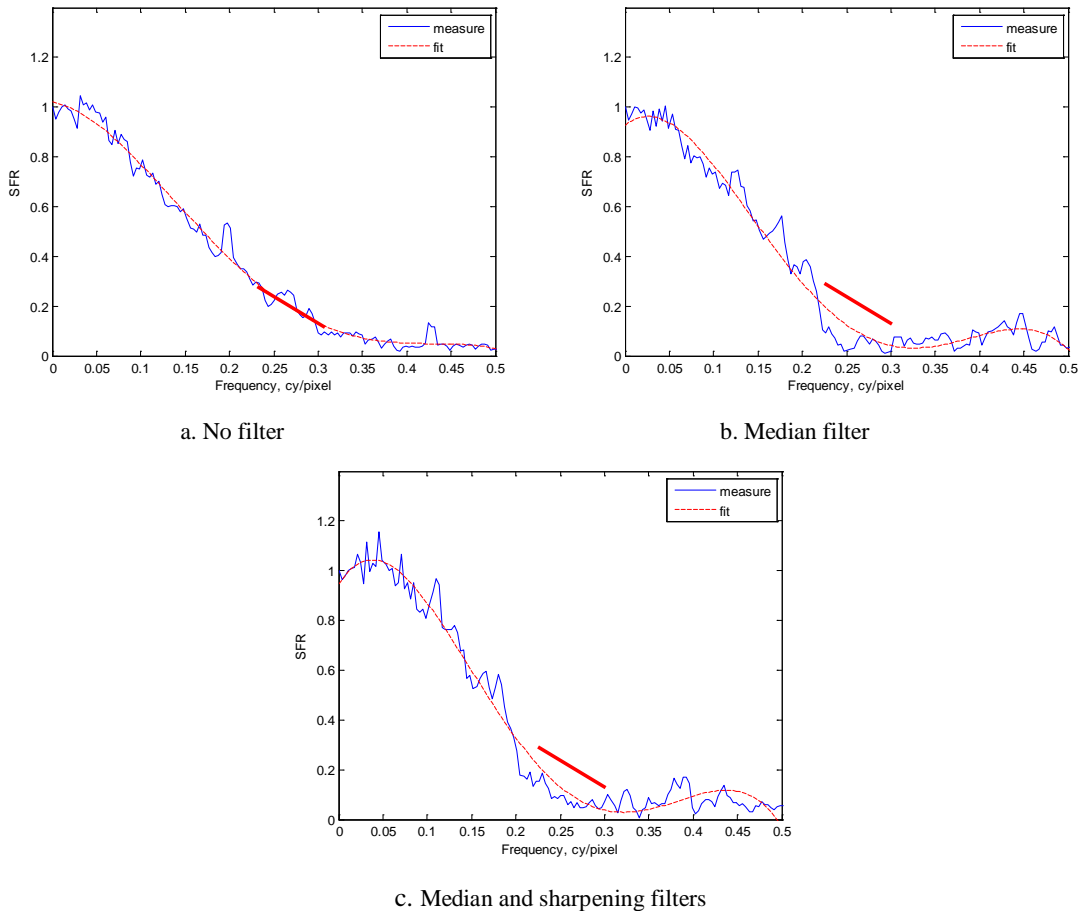


Figure 13: Results of the intrinsic SFR measurements for (a) Camera (ISO 400), (b) after (5x5) median filter and (c) after median and sharpening filters, with dead-leaves target

## Acknowledgements

We thank Sergio Goma and Kalin Atanassov for their contributions to this effort during discussions of the objectives, technical approaches, and results. Thanks also go to Penny Raile for permission to use and publish her *Zentangle Square 2* pattern.

## 6. REFERENCES

- [1] Burns, P. D., "Slanted-Edge MTF for Digital Camera and Scanner Analysis," Proc. PICS Conf., IS&T, 135-138 (2000).
- [2] Loebich, C., Wüller, D., Klingen, B., Jäger, A., "Digital Camera Resolution Measurement Using Sinusoidal Siemens Stars," Proc. SPIE 6502, 6502N (2007).
- [3] ISO 12233:2014, Photography -- Electronic still picture imaging -- Resolution and spatial frequency responses, ISO, (2014).
- [4] Cao, F., Guichard, F., and Hornung, H., "Measuring texture sharpness of a digital camera," Proc. SPIE 7250, 72500H (2009).
- [5] Kirk, L., Herzer, P., Artmann, U. and Kunz, D., "Description of texture loss using the dead leaves target: current issues and a new intrinsic approach," Proc. SPIE 9014, (2014).
- [6] Burns, P. D., "Refined Measurement of Digital Image Texture Loss," Proc. SPIE 8653, Image Quality and System Performance X, 86530H (2013).

## APPENDIX

### *Application of cross-spectrum to MTF Estimation*

The noise-power spectrum can be used to measure the MTF of a linear system. As in Fig. 1a the input,  $p(t)$ , and output,  $r(t)$  are related by a linear system with MTF,  $H$  and a noise source,  $n(t)$ . The output auto-spectrum is

$$\Phi_{rr}(f) = H^2(f)\Phi_{pp}(f) + \Phi_{nn}(f) \quad (1a)$$

The corresponding cross-spectrum is

$$\Phi_{pr}(f) = H(f)\Phi_{pp}(f) + \Phi_{pn}(f) \quad (2a)$$

So if we know the input signal (test target)  $p(t)$  and observe the output,  $r(t)$ , then we can solve Eq. (2a) for the MTF without the bias introduced by  $\Phi_{nn}$  because  $\Phi_{pn}(f) < \Phi_{nn}(f)$ . This is the method we will be using to estimate the image signal transfer.

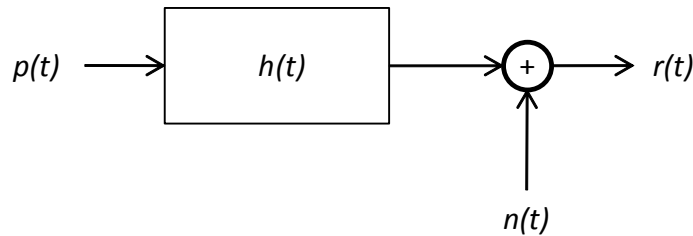


Figure 1a: Linear system with noise source